Quantitative study of hydration of C_3S and C_2S by thermal analysis

Evolution and composition of C–S–H gels formed

Sara Goñi · Francisca Puertas · María Soledad Hernández ·
Marta Palacios · Ana Guerrero · Jorge S. Dolado ·
Bruno Zanga · Fulvio Baroni

Abstract This research is part of a European project (namely, CODICE project), main objective of which is modelling, at a multi-scale, the evolution of the mechanical performance of non-degraded and degraded cementitious matrices. For that, a series of experiments were planned with pure synthetic tri-calcium silicate (C_3S) and bi-calcium silicate (C_2S) (main components of the Portland cement clinker) to obtain different calcium–silicate–hydrate (C–S–H) gel structures during their hydration. The characterization of those C–S–H gels and matrices will provide experimental parameters for the validation of the multi-scale modelling scheme proposed. In this article, a quantitative method, based on thermal analyses, has been used for the determination of the chemical composition of the C–S–H gel together with the degree of hydration and quantitative evolution of all the components of the pastes. Besides, the microstructure and type of silicate tetrahedron and mean chain length (MCL) were studied by scanning electron microscopy (SEM) and ^{29}Si magic-angle-spinning (MAS) NMR, respectively. The main results showed that the chemical compositions for the C–S–H gels have a CaO/SiO_2 M ratio almost constant of 1.7 for both C_3S and C_2S compounds. Small differences were found in the gel water content: the H_2O/SiO_2 M ratio ranged from 2.9 ± 0.2 to 2.6 ± 0.2 for the C_3S (decrease) and from 2.4 ± 0.2 to 3.2 ± 0.2 for the C_2S (increase). The MCL values of the C–S–H gels, determined from ^{29}Si MAS NMR, were 3.5 and 4 silicate tetrahedron, for the hydrated C_3S and C_2S, respectively, remaining almost constant at all hydration periods.

S. Goñi · F. Puertas · M. S. Hernández · M. Palacios ·
A. Guerrero
Instituto de Ciencias de la Construcción Eduardo Torroja
(IETcc) (CSIC), C/ Serrano Galvache, 4, 28033 Madrid, Spain

S. Goñi (✉) · F. Puertas · M. S. Hernández · M. Palacios ·
A. Guerrero · J. S. Dolado
Nanostructured and Eco-Efficient Materials for Construction
Unit, Associated Unit LABEIN-Tecnalia/CSIC.IETcc,
Madrid, Spain
e-mail: sgoni@ietcc.csic.es

J. S. Dolado
Centre for Nanomaterials Application in Construction
(NANOC), LABEIN-Tecnalia, Parque Tecnológico
de Bizkaia, C/ Geldo, 48160 Derio, Bilbao, Spain

B. Zanga · F. Baroni
Grupo CTG Italcementi, Via G. Camozzi, 124,
24121 Bergamo, Italy

Introduction

Portland cements are widely used in the world as building materials due to their great mechanical and chemical properties. These cements are constituted by clinker which is a polyphasic material including calcium silicates: C_3S (Ca_3SiO_5) or alite and C_2S (Ca_2SiO_4) or belite, calcium aluminate C_3A ($Ca_3Al_2O_6$) and calcium alumino-ferrites (C_4AF) at which calcium sulphates (mainly gypsum) and other supplementary cementitious materials (SCMs) are added [1]. The European standard for common cements (EN 197-1) recognizes 27 different cement materials.

CEM I according to European standard is constituted by clinker (95% wt) and gypsum or others materials (5% wt), and usually contain 50–70 wt% of alite (C_3S) and 5–30 wt% of belite. The characterization of anhydrous constituents and the hydrated products together with the calculation of hydration degree of each component over time clearly

constitute a solid experimental basis for assessing the evolution of this cement material and its properties. For this purpose numerous investigations on the hydration reactions of the C_3S and C_2S have been carried out [2–5], among others; nevertheless, recently researchers have taken up investigations, again due to the need to validate experimentally the models, which increasingly are being carried out on the Portland cement pastes and especially the advances in the characterization of the gel C–S–H (calcium–silicate–hydrate) [6–9]. The C_2S is characterized by a slow reaction of hydration that awards it specific properties. The interest for this phase is growing giving place to cement with high percentage of activated belite, named 'belite cements' [10].

Of the two products of C_3S and C_2S hydration, C–S–H gel and portlandite ($Ca(OH)_2$), the importance of the C–S–H gel deserves special mention from the points of view of its engineering properties, elasticity and durability [11–15]. Therefore, it is well known that the composition and internal structure of C–S–H gels define both the mechanical and durable behaviour of the final cementitious materials. For these specific reasons, it is necessary to characterize the C–S–H gel formed during the hydration of cements and calcium silicate phases, and the changes during the service life of concrete structures. In spite of the efforts and great amount of studies carried out [11–27], there are still questions on its internal structure at a nanometric scale and its effect in the properties of the concrete.

There are experimental evidences confirming the value of 1.7 for the CaO/SiO_2 M ratio of the gel C–S–H [21]. In the case of the water content of the gel, the H_2O/SiO_2 M ratio changes depending on the relative humidity (RH), obtaining a value of 4 for the saturated condition (which includes the structural water between the layers, the water adsorbed on the layers and the water in pores); 2.1 for 11% RH (which includes the structural water contained between the sheets of the gel), and about 1.4 after a strong drying process at vacuum (D-drying method) or by heating at 105 °C [1]. The loss of the gel water due to drying has important consequences on the dimensional stability, shrinkage and elasticity module [12–15].

This research is part of a European project (namely CODICE project) [28], main objective of which is the multi-scale modelling of the evolution of the mechanical performance of non-degraded and degraded cementitious matrices. For this purpose, a series of experiments were planned with pure synthetic tri-calcium silicate (C_3S) and bi-calcium silicate (C_2S) (main components of the Portland cement) to obtain different C–S–H gel structures during their hydration. The characterization of those C–S–H gels and matrices will provide experimental parameters for the validation of the multi-scale modelling scheme proposed.

Thermal analysis is a useful tool for quantifying different parameters of interest in the building materials, i.e. for evaluating the pozzolanic activity of waste additions to Portland clinker [29–31], for evaluating the effect of alkaline hydrothermal activation of fly ash belite cement [10] or kinetic equations of alkaline activation of blast furnace slag [32] and for quantitative determination of the chemical composition of the C–S–H gel and degree of hydration, which is the main aim of this study.

In this article, a quantitative method, based on thermal analyses, has been used for the determination of the chemical composition of the C–S–H gel together with the degree of hydration and quantitative evolution of all the components of the pastes. Besides, the microstructure and type of silicate tetrahedron and mean chain length (MCL) were studied by scanning electron microscopy (SEM) and ^{29}Si MAS NMR, respectively.

Experimental

Materials

Triclinic (T1) tri-calcium silicate, (T1-Ca_3SiO_5, C_3S), and bicalcium silicate (β-Ca_2SiO_4, C_2S) were synthesized from commercially available lab chemicals with a purity exceeding 99%: SiO_2 (Aerosil 380 Degussa with a purity of 99.8%), $CaCO_3$ (Prolabo RP Normapur with a purity of 99.5%) and B_2O_3 (Prolabo RP Normapur with a purity considered as 100%). Stoichiometric mixes with CaO to SiO_2 M ratios of 3:1 and 2:1 have been prepared, for the C_3S and C_2S, respectively. In the case of the β-C_2S preparation, B_2O_3 have been used as stabiliser. The mixes have been homogenised by adding water, and mixed by means of a Hobart mixer for about 15 min. The obtained slurry were kneaded into bars and put on a platinum support. After a preliminary drying at 110 °C for 12 h, the material was put in a high temperature furnace. For both preparations, an initial pre-heating was necessary to avoid the violent CO_2-gas evaporation from $CaCO_3$. The sintering protocols were the following:

C_3S: 80 min of heating ramp to 1000 °C, then holding for 40 min; 1.5 h of heating ramp to 1550 °C, then holding for 2 h.
C_2S: 110 min of heating ramp to 1000 °C, then holding for 40 min; 70 min of heating ramp to 1450 °C, then holding for 3 h.

The quenching of the material was performed using an air stream. The resulting material was manually ground to have a powder that passes 40 µm and a small amount of this powder have been analysed by X-ray powder diffraction; the determination of the free lime was performed by the wet chemical method (Franke method [33]). For the

C$_3$S preparation, the sintering process is repeated following the same sintering protocol, until the free lime content resulted to be negligible.

The products resulting from this process were identified using X-ray diffraction as the triclinic T1 form, in the case of C$_3$S, and as β-C$_2$S. The particle size distribution pattern (Fig. 1) presents the following particle size populations: one around 1 μm and the bigger at 10 μm, for the synthesized C$_3$S powder; and around 1.5, 8, 12 and 37 μm for the C$_2$S.
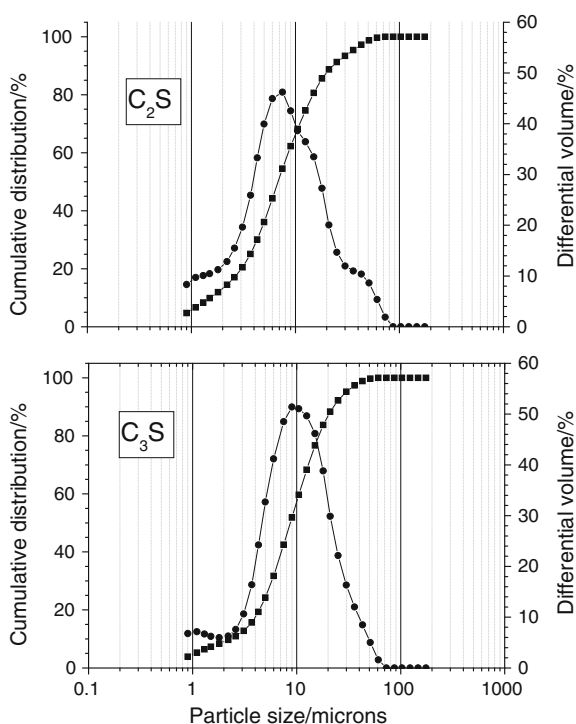
Paste preparation

Synthetic C$_3$S and C$_2$S pastes, prepared by mixing the powder with distilled and decarbonated water at a water/solid ratio of 0.4, were cast in $1 \times 1 \times 6$-cm^3 moulds and consolidated by tapping. All these operations were conducted in an inert N$_2$ atmosphere inside an 'Atmosbag'. The specimens were removed from the moulds 24 h after casting, wrapped in aluminium foil and stored in containers with distilled and decarbonated water at $\sim 100\%$ RH. At the end of each hydration period, i.e. 1, 3, 7 and 28 days for C$_3$S and 7, 28 and 90 days for C$_2$S (for C$_2$S pastes, longer curing times have been evaluated due to its slower hydration reaction), the specimens were crushed and the powder dried with acetone (45 s) and ethanol (15 s) and put into the atmosbag until the following tests. In order to prevent sample carbonation, the experiment was conducted in an

inert atmosphere wherever possible. Immediately prior to characterization analysis, the samples were vacuum dried in desiccators for 1 h at ambient temperature.

Instrumentation

Thermal analyses were carried out with a Netxsch STA 409 simultaneous thermal analyser fitted with a Data Acquisition Systems 414/1 programmer. Samples (maximum amount accommodated by the crucible) were heated to 1050 °C at a rate of 4 °C min^{-1} in an inert atmosphere (N$_2$) and subsequently cooled at 10 °C min^{-1}. ^{29}Si MAS NMR was likewise used to monitor synthetic phase hydration. As in the anhydrous phases, the positions occupied by the ^{29}Si atoms were found with solid nuclear magnetic resonance (MAS NMR) techniques, using a Bruker MSL400 spectrophotometer operating at 79.49 MHz. Tetramethyl silane (TMS) was used as the external standard for the ^{29}Si spectra. Spectral analyses were performed using Winfit software (Bruker). Component intensity, position and line width were determined with a standard interactive least squares method. The scanning electron microscope used was a JOEL JSM 5400 model, fitted with a LINK-ISIS EDX microanalyser. The particle size distribution of the powders was measured by laser granulometry analysis (Sympatec Helos 12 KA instrument fitted with: an He/Ne, 5-mW light source) using isopropyl alcohol as dispersant and ultrasound to disagglomerate the particles before the measurement.

Results and discussion

Thermal analysis

The experimental data obtained from thermogravimetric analysis (TG) allowed us to quantify the phases formed during hydration of C$_3$S and C$_2$S: portlandite (Ca(OH)$_2$) and C–S–H gel. In addition, it has been possible to estimate the hydration degree (α), the stoichiometry of the hydration reactions, the mass balance of the starting and final products for the two C$_3$S and C$_2$S phases and the chemical composition of the C–S–H gel.

The TG and differential scanning calorimetry (DSC) curve profiles of the hydrated samples were similar to those shown in Fig. 2, which shows the thermal decomposition of C$_3$S and C$_2$S pastes after 28 days of hydration. As can be seen, a continuous mass loss between 25 and 350 °C is observed in the TG curves, which is due to the release of water molecules from the C–S–H gel decomposition; a second and well-defined mass loss is produced between 350 and 450 °C, which is due to the water molecules released from the portlandite decomposition, and a very small and continuous mass loss from about 550–600 to
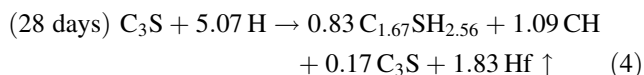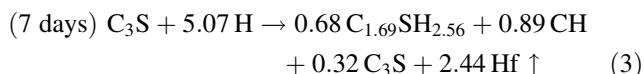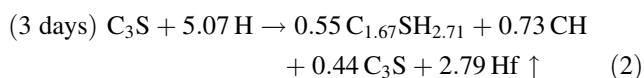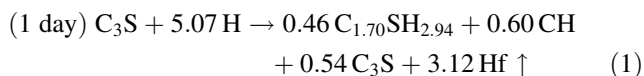

Fig. 1 Particle size distribution for anhydrous C$_3$S and C$_2$S
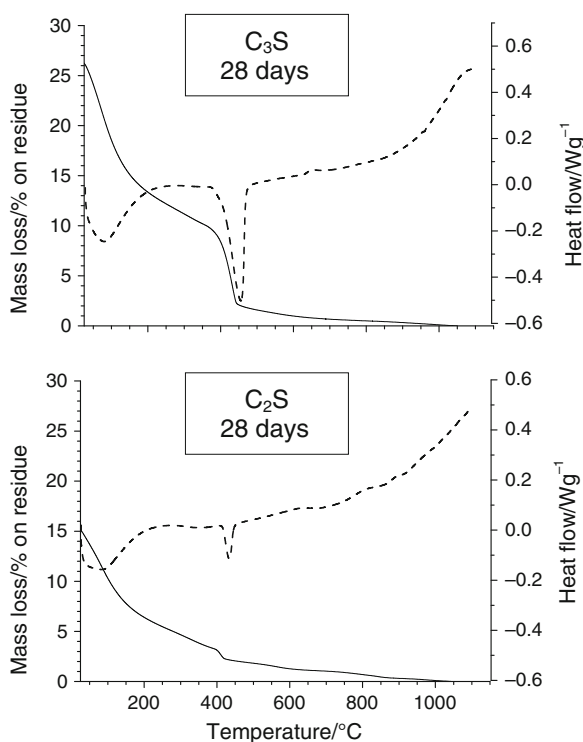
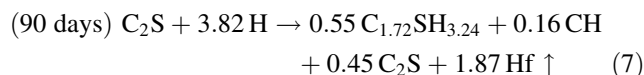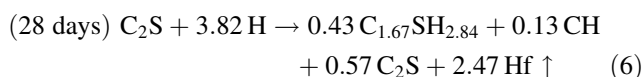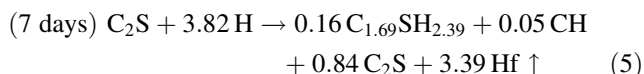**Fig. 2** TG and DSC curves of C_3S and C_2S pastes hydrated for 28 days

1050 °C due to the release of the CO_2 molecules from possible carbonation or weathering of samples [2].

These mass losses produce endothermic peaks in the corresponding DSC curves, which are centred at 75 and 413–433 °C, respectively. On the basis of the TG data, the following adjusted hydration reactions can be raised at every step studied:

For C_3S:

$$(1\ \text{day})\ C_3S + 5.07\,H \rightarrow 0.46\,C_{1.70}SH_{2.94} + 0.60\,CH \\ + 0.54\,C_3S + 3.12\,Hf \uparrow \quad (1)$$

$$(3\ \text{days})\ C_3S + 5.07\,H \rightarrow 0.55\,C_{1.67}SH_{2.71} + 0.73\,CH \\ + 0.44\,C_3S + 2.79\,Hf \uparrow \quad (2)$$

$$(7\ \text{days})\ C_3S + 5.07\,H \rightarrow 0.68\,C_{1.69}SH_{2.56} + 0.89\,CH \\ + 0.32\,C_3S + 2.44\,Hf \uparrow \quad (3)$$

$$(28\ \text{days})\ C_3S + 5.07\,H \rightarrow 0.83\,C_{1.67}SH_{2.56} + 1.09\,CH \\ + 0.17\,C_3S + 1.83\,Hf \uparrow \quad (4)$$

For C_2S:

$$(7\ \text{days})\ C_2S + 3.82\,H \rightarrow 0.16\,C_{1.69}SH_{2.39} + 0.05\,CH \\ + 0.84\,C_2S + 3.39\,Hf \uparrow \quad (5)$$

$$(28\ \text{days})\ C_2S + 3.82\,H \rightarrow 0.43\,C_{1.67}SH_{2.84} + 0.13\,CH \\ + 0.57\,C_2S + 2.47\,Hf \uparrow \quad (6)$$

$$(90\ \text{days})\ C_2S + 3.82\,H \rightarrow 0.55\,C_{1.72}SH_{3.24} + 0.16\,CH \\ + 0.45\,C_2S + 1.87\,Hf \uparrow \quad (7)$$

where H is the water used for mixing, CH stands for portlandite, which has been quantified from the water molecules released between 350 and 450 °C and Hf is free water: i.e. the difference between the total water used for mixing and the water molecules combined with the solid hydrated phases (portlandite (CH) and C–S–H gel). Let us note that Hf representing the excess of water used in mixing and necessary for allowing a good workability is evaporated in the drying process, and is the cause of the free space (capillary porosity).

The portlandite content has been used for the calculation of the hydration degree (α) taking into account the maximum values of 1.3 and 0.3 mol of portlandite per mole of C_3S and C_2S, respectively [1, 3, 7]; the unreacted C_3S and C_2S were calculated from the hydration degree: $(1 - \alpha)$.

In the case of the stoichiometry of the C–S–H gel, the water molecules were experimentally measured from the differences obtained between the mass loss at 600 °C and the mass loss from the water molecules of portlandite decomposition; the CaO and SiO_2 molecules were adjusted by mass balance between the initial products of the reactions and those of the second term of reactions.

The CaO/SiO_2 M ratio in the C–S–H gels formed is maintained almost constant independent of the duration of hydration; however, the value of the H_2O/SiO_2 M ratio, in the case of C_3S, decreases lightly over hydration: 2.9 ± 0.2–2.6 ± 0.2 over a period from 1 to 28 days (in fact is practically constant taking into account the dispersion of ± 0.2, corresponding to the standard deviation of '5' sample analyses). These values are in good agreement with those reported by Costoya [9] for the C–S–H gel obtained from the hydration of synthetic pure C_3S of 7 μm of particle size; in this case, the hydration was stopped by drying with isopropanol organic solvent. Nevertheless, in the case of the C_2S, the value of the H_2O/SiO_2 M ratio of the C–S–H gel ranged from 2.4 ± 0.2 to 3.2 ± 0.2 over a period from 7 to 90 days of hydration. At the moment, we have no explanation for this behaviour, but the value of 3.2 is close to that reported by Costoya for the aforementioned C_3S taking into account the dispersion of ± 0.2 of the data.

In Fig. 3, the mass fractions of all the components of the matrices, calculated from the above adjusted reactions, are presented. In this figure, the differences among the matrices of C_3S and C_2S are clearly shown.

The rates of the hydration reactions were calculated from the regression equations of the curves of Fig. 4, where the evolutions, with hydration time, of portlandite, C–S–H gel and hydration degree are presented.

All the curves can be pretty well adjusted to a direct semi-logarithmic function. In the case of the portlandite,

both the amount formed and its rate of gain (the slope of the regression equation) is considerably higher for the C_3S than those of C_2S. After 90 days of hydration, the amount of portlandite formed is 5.1% for the C_2S and 25.2% for the C_3S after 28 days. The rate of portlandite formation is 2.5 times higher for C_3S than that of C_2S. In the case of C_2S, an induction period of 2 days before start of hydration can be deduced from the regression equation. The amount of C–S–H gel formed at early ages is considerably higher for the C_3S in comparison with that of C_2S; nevertheless, the difference diminishes at later stages of hydration, at which the C–S–H gel was 52.6 (28 days) and 48.7% (90 days) for C_3S and C_2S, respectively; again, an induction period of 2 days is produced, in the case of C_2S. Nevertheless, the rate of C–S–H gel gain is two times higher in the case of the C_2S in comparison with that of C_3S. If the hydration degree is taken into account, then the difference in the rates of hydrations diminishes, and a similar induction period of 2 days is observed for the C_2S. It should be mentioned that, in the case of C_3S, the hydration degree values obtained from thermal analysis coincide pretty well with those obtained from NMR results (see Table 2).

SEM

The microstructure of both C_3S and C_2S matrices are given in Figs. 5 and 6. The microstructure is compacted as hydration progresses, as can be observed in Fig. 5a–c, where the microstructural changes for the C_3S matrices are clearly shown: an open structure with C–S–H particles appearing as aggregates of globular morphology and portlandite crystals as fine plates of smooth surfaces can be detected after 3 days of hydration (a). The size and amount of portlandite crystals increased as hydration time increased, appearing integrated in the microstructure after 28 days (compare Fig. 5a–c). By this period, the aggregates of globules of C–S–H almost disappeared and a more
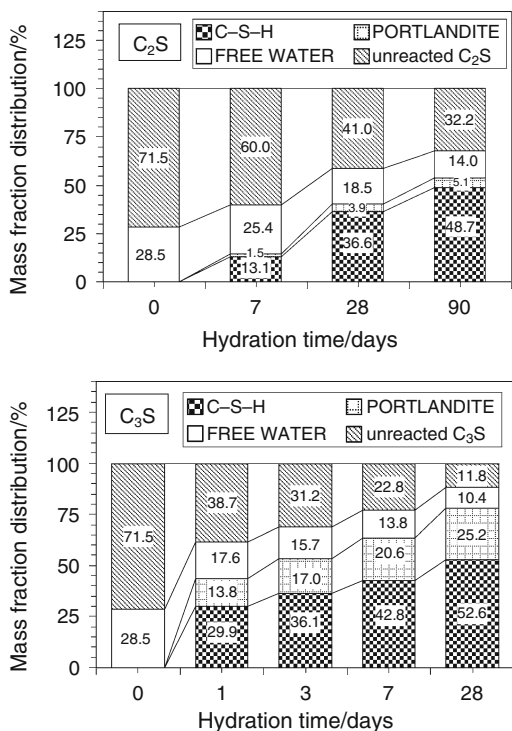

Fig. 3 Mass fraction distribution of all the components of C_3S and C_2S pastes, determined from quantitative TG results
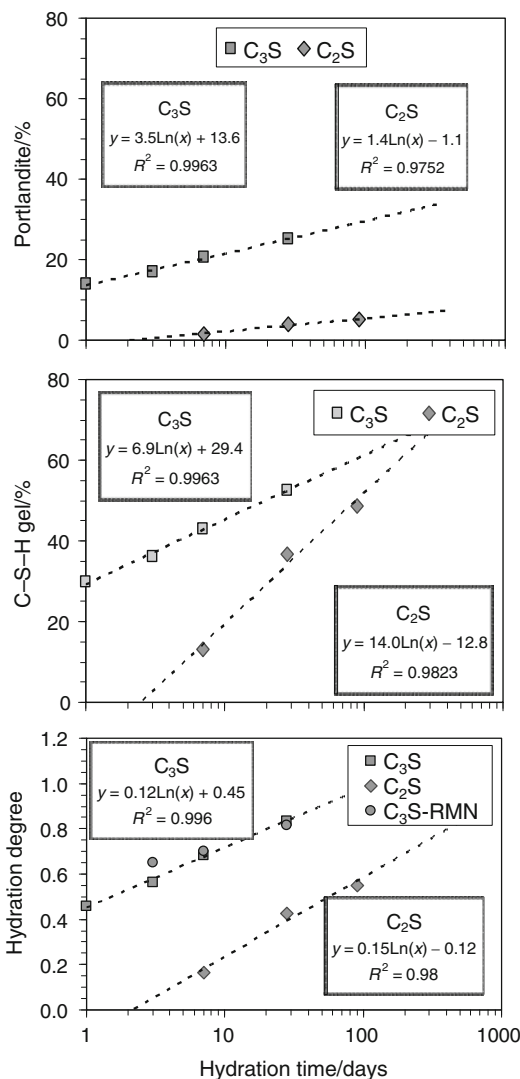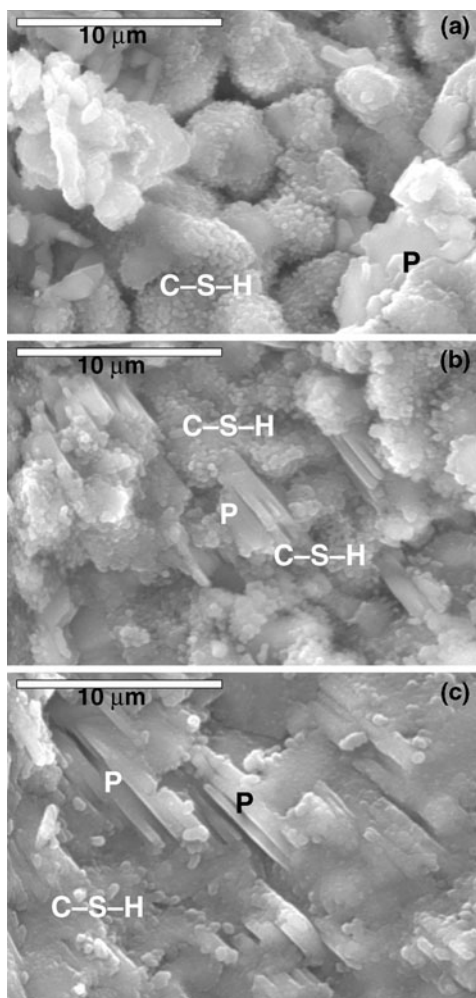

Fig. 4 Evolution of portlandite, C–S–H gel and hydration degree with hydration time: C_3S and C_2S pastes

**Fig. 5** SEM images of the microstructure of hydrated C_3S: **a** 3 days, **b** 7 days, **c** 28 days

compact microstructure is detected (c). The main differences observed in the microstructure of hydrated C_2S (Fig. 6) are: the less amount of portlandite crystals, which after 7 days (Fig. 6a) does not appear; the aspect of the C–S–H gel, and the less compact microstructure even after 28 days of hydration (compare Figs. 5c and 6b).

Magic angle spinning (MAS), nuclear magnetic resonance (NMR)

The ^{29}Si MAS NMR spectra over 28 days of hydration of both C_3S and C_2S are shown in Fig. 7. The deconvolution data for all the hydration times studied are given in Table 1. The ^{29}Si MAS NMR spectra for the C_3S pastes studied had six signals ranging from −69.0 to −74.7 ppm, attributable to isolated Q^0 tetrahedron present in anhydrous C_3S [34]. The three signals observed at around −79.0, −82.0 and −85.0 ppm were attributed, respectively, to Q^1, Q^{2B} and Q^2 Si units in the C–S–H gel [35].
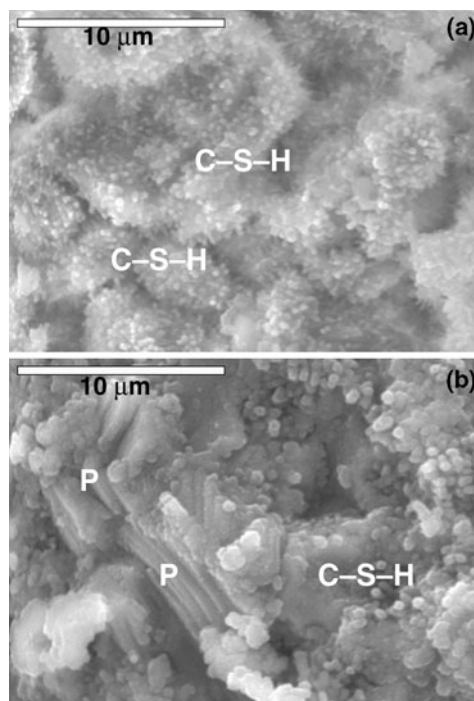
Fig. 6 SEM images of the microstructure of hydrated C_2S: **a** 7 days, **b** 90 days
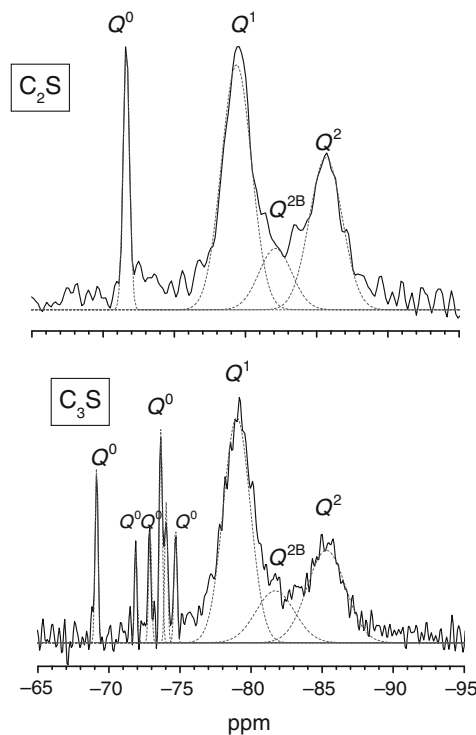
Fig. 7 ^{29}Si MAS NMR spectra for 28-days C_3S- and C_2S-hydrated pastes

The percentages of the Si units given in Table 2 and the mathematical Eq. 8 proposed by [36], which is, in turn, an adaptation of Richardson's equation [16, 37], were used to

Table 1 ^{29}Si MAS NMR spectra for C₃S and C₂S hydrated pastes (deconvolution data)

Sample	Time/days	Q^0						Q^1 (end chain)	Q^{2B}	Q^2
C₃S	3									
	ppm	−69.3	−72.0	−73.0	−73.8	−74.2	−74.8	−79.2	−82.3	−85.3
	W	0.25	0.25	0.25	0.25	0.25	0.25	2.80	3.0	3.0
	I (%)	7.6	4.2	4.4	9.3	5.3	4.5	37.7	9.1	17.9
	7									
	ppm	−69.3	−72.0	−73.0	−73.8	−74.2	−74.8	−79.2	−82.0	−85.3
	W	0.24	0.24	0.24	0.24	0.24	0.24	2.30	2.70	2.70
	I (%)	6.0	3.6	3.9	8.1	4.7	3.8	41.3	9.9	18.7
	28									
	ppm	−69.2	−71.9	−72.9	−73.7	−74.1	−74.7	−79.0	−81.7	−85.3
	W	0.27	0.27	0.27	0.27	0.27	0.27	2.30	2.70	2.70
	I (%)	3.8	2.0	2.5	4.8	2.8	2.5	44.8	12.3	24.5
C₂S	7									
	ppm		71.7					−79.7	−82.8	−85.7
	W	–	0.36	–	–	–	–	2.30	2.70	2.70
	I (%)		28.7					36.9	11.3	23.2
	28									
	ppm		−71.6					−79.4	−82.3	−85.8
	W	–	0.27	–	–	–	–	2.30	2.70	2.70
	I (%)		8.1					46.8	12.4	32.7
	90									
	ppm		71.8					−79.3	−82.5	−85.6
	W	–	−0.13	–	–	–	–	2.40	2.60	2.60
	I (%)		9.1					43.1	12.5	35.3

W width, *I* integral

find the MCL of the C–S–H gel formed at each hydration period concerned.

$$MCL = [(2(Q^1 + Q^2(0Al) + Q^{2B}(0Al))/Q^1] \quad (8)$$

As the data in Tables 1 and 2 show, the percentages of the Si Q^1, Q^{2B} and Q^2 units associated with C–S–H gel increased over time. This rise was associated with the degree of reaction, which climbed from 65 to 82% between the periods of 3 and 28 days (Table 2). As was mentioned earlier, these data are very similar to the TG findings.

Moreover, in all the pastes studied, the MCL remained essentially constant at all hydration periods with a value about 3.5. Interestingly, this value can be explained in terms of an equal population of dimeric jennite- and pentameric tobermorite-like structures, something which fits well with the structural models of C–S–H gel [1, 11] and is consistent with a C/S ratio close to 1.7, as the TG results have also concluded. In the case of the C–S–H gel of hydrated C₂S, the corresponding value of MCL was 4, which is consistent with a population of 33% of dimeric jennite and 67% of pentameric tobermorite.

The ^{29}Si MAS NMR spectra for the C₂S studied contained one signal at −71.6 ppm, attributed to the isolated

Q^0 tetrahedra present in anhydrous C₂S [34]; in the C₂S pastes, the signals observed at −79.0, −82.0 and −85.0 ppm were attributed, respectively, to the Q^1, Q^{2B} and Q^2 Si units in the C–S–H gel.

Contrary to the C₃S pastes, the NMR technique was less satisfactory for estimating the degree of hydration for the C₂S pastes giving higher values than those of the TG method. The reason for this is unknown, but it could be associated with the data collection which is confined to a too small area of the Si Q^0 unit, which is associated with the anhydrous phase. Under these circumstances, the degree of reaction would lead to extremely high values (72 and 92% at 7 and 28 days, respectively) for samples with notoriously low reactivity. However, further investigation is needed to clarify this issue.

Conclusions

- From the TG results, it has been possible to quantify important parameters of the C₃S and C₂S hydration reactions, such as the hydration degree, the stoichiometry of the hydration reactions, the mass balance of the

Table 2 Further deconvolution data for ^{29}Si MAS NMR spectra of C$_3$S- and C$_2$S-hydrated pastes: degree of hydration (α) and MCL

Sample	Time/days	$\alpha = (1 - (Q^\circ)) \times 100$	MCL	$\sum Q^2/Q_{\text{total}}$	$\sum Q^2/Q^1$
C$_3$S	3	65	3.4	0.42	0.71
	7	70	3.4	0.41	0.69
	28	82	3.8	0.47	0.90
C$_2$S	7	71	3.9	0.48	0.93
	28	92	3.9	0.49	0.96
	90	91	4.2	0.52	1.10

starting and final products and the chemical composition of the C–S–H gel.

- The value of the H$_2$O/SiO$_2$ M ratio, in the case of C$_3$S, decreases slightly over hydration: from 2.9 ± 0.2 to 2.6 ± 0.2 from 1 to 28 days. Nevertheless, in the case of the C$_2$S, the value of the H$_2$O/SiO$_2$ M ratio of the C–S–H gel ranged from 2.4 ± 0.2 to 3.2 ± 0.2 from 7 to 90 days of hydration.

- From the regression equations of the hydration reactions, an induction period of 2 days is established for the C$_2$S.

- A good agreement between the hydration degrees, obtained from TG and NMR techniques, has been achieved only in the case of C$_3$S pastes.

- The value of 3.5 for the MCL of the C–S–H gel of hydrated C$_3$S is consistent with an equal population of dimeric jennite- and pentameric tobermorite-like structures, which is also consistent with a C/S ratio close to 1.7, as the TG results have also concluded. In the case of the C–S–H gel of the hydrated C$_2$S, the corresponding value of MCL was 4, which is consistent with a population of 33% of dimeric jennite and 67% of pentameric tobermorite.

References

1. Taylor HFW. Cement chemistry. London: Academic Press; 2nd ed. Telford Publishing, 1997.
2. Taylor HFW, Turner AB. Reactions of tricalcium silicate paste with organic liquids. Cem Concr Res. 1987;17:613–23.
3. Fujii K, Kondo W. Kinetics of the hydration of tricalcium silicate. J Am Ceram Soc. 1974;57(11):492–7.
4. Daimon M, Ueda S, Kondo R. Morphological study on hydration of tricalcium silicate. Cem Concr Res. 1971;1:391–401.
5. de Jong JGM, Stein HN, Stevels JM. Hydration of tricalcium silicate. J Appl Chem. 1967;17:246–50.
6. Bishnoi S, Scrivener KL. Studying nucleation and growth kinetics of alite hydration using μic. Cem Concr Res. 2009. doi:10.1016/j.cemconres.2009.07.004.
7. Bishnoi S, Scrivener KL. μic: a new platform for modelling the hydration of cements. Cem Concr Res. 2009;39:266–74.
8. Bishnoi S. Vector modelling of hydrating cement microstructure and kinetics. Thèse no 4093. École Polytechnique Fédérale de Lausanne; 2008.
9. Costoya Fernandez MM. Effect of particle size on the hydration kinetics and microstructural development of tricalcium silicate. Thèse n° 4102. École Polytechnique Fédérale de Lausanne; 2008.
10. Goñi S, Guerrero A. Study of alkaline hydrothermal activation of belite cements by thermal analysis. J Therm Anal Calorim. 2010;99(2):471–7.
11. Taylor HFW. Proposed structure for calcium silicate hydrate gel. J Am Ceram Soc. 1986;69(6):464–7.
12. Powers TC, Brownyard TL. Studies of the physical properties of hardened Portland cement paste. Skokie, IL: Portland Cement Association R&D Bull. 22. Reprinted from J Am Concr Inst. 1946;18(2):101–32 and 1948;8(5):549–602.
13. Powers TC. Physical properties of cement paste. Proceedings of the Fourth International Symposium on Chemistry of Cement, Washington, USA; 1960. p. 577–613.
14. Feldman RF, Sereda PJ. A model for hydrated Portland cement paste as deduced from sorption length change and mechanical properties. Mater Struct. 1968;1(6):509–20.
15. Feldman RF, Sereda PJ. A new model for hydrated Portland cement and its practical implications. Eng J Can. 1970;53(8/9):53–9.
16. Richardson IG. Tobermorite/jennite- and tobermorite/calcium hydroxide-based models for the structure of C–S–H: applicability to hardened pastes of tricalcium silicate, β-dicalcium silicate, Portland cement, and blends of Portland cement with blast-furnace slag, metakaolin, or silica fume. Cem Concr Res. 2004;34:1733–77.
17. Jennings HM. A model for the microstructure of calcium silicate hydrate in cement paste. Cem Concr Res. 2000;30:101–16.
18. Tennis PD, Jennings HM. A model for two types of C–S–H in the microstructure of Portland cement pastes. Cem Concr Res. 2000;30:855–63.
19. Constantinides G, Ulm F-J. The effect of two types of C–S–H on the elasticity of cement based materials: results from nanoindentation and micromechanical modelling. Cem Concr Res. 2004;34:67–80.
20. Thomas JJ, Jennings HM. A colloidal interpretation of chemical aging of the C–S–H gel and its effects on the properties of cement paste. Cem Concr Res. 2006;36:30–8.
21. Allen AJ, Thomas JJ, Jennings HM. Composition and density of nanoscale calcium–silicate–hydrate in cement. Nat Mater. 2007;6:311–6.
22. Constantinides G, Ulm F-J. The nanogranular nature of C–S–H. J Mech Phys Solids. 2007;55:64–90.
23. Jennings HM. Refinements to colloid model of C–S–H in cement: CM-II. Cem Concr Res. 2008;38:275–89.
24. Dolado JS, Griebel M, Hamaekers J. A molecular dynamic study of cementitious calcium silicate hydrate (C–S–H) gels. J Am Ceram Soc. 2007;90(12):3938–42.
25. Manzano H, Dolado JS, Griebel M, Hamaekers J. A molecular dynamics study of the aluminosilicate chains structure in Al-rich calcium silicate hydrated (C–S–H) gels. Phys Status Solidi A. 2008;205(6):1324–9.
26. Vandamme M, Ulm F-J, Fonollosa P. Nanogranular packing of C–S–H at substochiometric conditions. Cem Concr Res. http://dx.doi.org/10.1016/j.cemconres.2009.09.017.
27. Pellenq RJM, Kushim A, Shahsavari R, Van Vliet KJ, Buehler MJ, Yip S, Ulm F-J. A realistic molecular model of cement hydrates. www.pnas.org_cgi_doi_10.1073_pnas.0902180106.

28. **CO**mputationally **D**riven design of **I**nnovative **CE**ment-based materials (CODICE) project—contract NMP3-SL-2008-214030. www.codice-project.eu.

29. Cherem da Cunha L, Gonzalves JP, Büchler PM, Dweck J. Effect of metakaolin pozzolanic activity in the early stages of cement type ii paste and mortar hydration. J Therm Anal Calorim. 2008;92:115–9.

30. Pacewska B, Wiliñska I, Bukowska M. Calorimetric investigations of the influence of waste aluminosilicate on the hydration of different cements. J Therm Anal Calorim. 2009. doi:10.1007/s10973-008-9668-9.

31. Vessalas K, Thomas PS, Ray AS, Guerbois J-P, Joyce P, Haggman J. Pozzolanic reactivity of the supplementary cementitious material pitchstone fines by thermogravimetric analysis. J Therm Anal Calorim. 2009. doi:10.1007/s10973-008-9708-5.

32. Fernández-Jiménez A, Puertas F, Arteaga A. Determination of kinetic equations of alkaline activation of blast furnace slag by means of calorimetric data. J Therm Anal Calorim. 1998;52:945–55.

33. Pressler EE, Brunauer S, Kantro DL. Investigation of the Franke method of determining free calcium hydroxide and free calcium oxide. Anal Chem. 1956;28(5):896–902.

34. Skibsted J, Hjorth J, Jakobsen HJ. Correlation between ^{29}Si NMR chemical shifts and mean Si–O bond lengths for calcium silicates. Chem Phys Lett. 1990;172(3–4):279–83.

35. Kirkpatrick RJ, Cong X. An introduction to ^{27}Al and ^{29}Si NMR spectroscopy of cements and concretes. In: Colombet P, Grimmer A, editors. Application of NMR spectroscopy to cement science. Amsterdam: Gordon & Breach; 1994. p. 55–76.

36. García-Lodeiro I. Compatibilidad de geles cementantes C-S-H y N-A-S-H. Estudios en muestras reales y en polvos sintéticos. Tesis Doctoral. Universidad Autónoma de Madrid; 2008.

37. Richardson IG. The nature of C–S–H in hardened cements. Cem Concr Res. 1999;29:1131–47.